BIOCHEMISTRY
including biophysical chemistry & molecular biology

Article

pubs.acs.org/biochemistry

# Tuning Cooperativity on the Free Energy Landscape of Protein Folding

Pooja Malhotra and Jayant B. Udgaonkar*

National Centre for Biological Sciences, Tata Institute of Fundamental Research, Bengaluru 560065, India

Supporting Information

**ABSTRACT:** Understanding the origin of the cooperativity seemingly inherent in a folding or unfolding reaction has been a major challenge. In particular, the relationship between folding cooperativity and stability is poorly understood. In this study, native state hydrogen exchange in conjunction with mass spectrometry has been used to explore the free energy landscape accessible to the small protein monellin, when the stability of the protein is varied. Mass distributions obtained in the EX1 limit of exchange have allowed a direct distinction between correlated (cooperative) and uncorrelated (noncooperative) structure-opening processes. Under conditions where the native protein is maximally stable, a continuum of partially unfolded states is gradually sampled before the globally unfolded state is transiently sampled. Under conditions that stabilize the unfolded state of the protein, the slowest structure-opening reactions leading to complete unfolding become cooperative. The present study provides experimental evidence for a gradual uphill unfolding transition on a very slow time scale, in the presence of a large free energy difference between the native and unfolded states. The results suggest that the cooperativity that manifests itself in protein folding and unfolding reactions carried out in the presence of denaturant might merely be a consequence of the effect of the denaturant on the unfolded state and transition state stabilities.

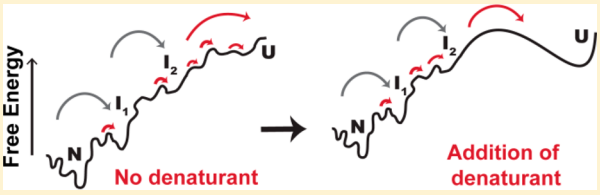


Energy landscape theory suggests that entropy−enthalpy compensation during protein folding may occur in a manner that results in many small ($\sim k_BT$) distributed barriers between the native (N) and unfolded (U) states.[1,2] On the resultant rugged free energy landscape, protein folding or unfolding would proceed via a continuum of states, in a gradual manner. For several proteins, there is now substantial experimental evidence for gradual unfolding[3,4] and folding,[5,6] including downhill folding.[7,8] Changes in the stabilities of N and U can affect the cooperativity of the transition (Figure 1) and can potentially cause a switch from a cooperative two-state process to a one-state gradual transition. Hence, factors that affect the stabilities of the ground states may modulate the cooperativity of the process. While the presence of a large barrier may prevent misfolding to aggregation prone states, the absence of a dominant barrier leads to the coexistence of multiple conformations which can be important for protein function.[9,10] It is therefore important to understand the cooperativity of folding and unfolding transitions, and the factors that modulate it.

Delineation of the degree of ruggedness in the energy landscape of a protein relies on the use of an appropriate probe and upon the experimental conditions. Under most experimental conditions, either N or U is the most stable species, and the interconversion between them appears to be dominated by a large free energy barrier. Consequently, folding and unfolding reactions appear to be "two-state", all-or-none reactions in which high energy intermediates are populated to too small an extent to be detected. Structural information on sparsely populated intermediate forms can, however, be obtained by the

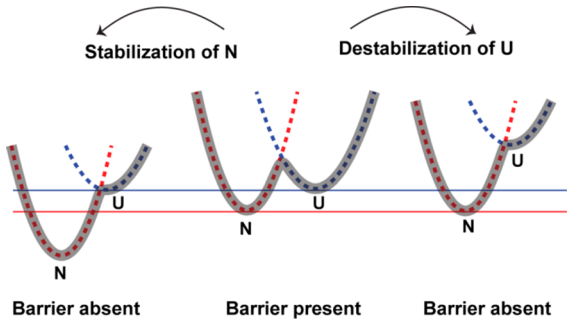


**Figure 1.** Modulation of the free energy surface describing protein unfolding and folding. A barrier limited transition (middle panel) can become barrierless due to a stabilization of the N state (left panel) or destabilization of the U state (right panel). The N and U energy wells are shown by the red and dark blue dashed lines, respectively. The position of the transition state along the reaction coordinate is given by the point at which the native and unfolded wells intersect each other. The resultant free energy surface (gray solid line) is determined as $-\ln[\exp\{-G_N(x)\} + \exp\{-G_U(x)\}]$, where $G_N(x)$ and $G_U(x)$ are the parabolic free energy wells shown for N and U, respectively, and $x$ is the horizontal variable. The left and right panels are indicative of unfolding reactions that would be completely uphill. The figure was inspired by Figure 6 in ref 66.

**Received:** March 7, 2015
**Revised:** May 16, 2015
**Published:** May 18, 2015





DOI: 10.1021/acs.biochem.5b00247
*Biochemistry* 2015, 54, 3431−3441

use of high resolution probes such as NMR,[11] as well as the native-state thiol labeling[12−14] and native-state hydrogen exchange (HX) methodologies. Native state HX can detect transient opening motions of the protein, from fast fluctuations that expose very localized structure to very slow unfolding events that expose the core of the protein.[15] Moreover, HX monitored by mass spectrometry (HX-MS) provides the time evolution of the population distributions of various species,[16] which allows a "two-state" transition to be distinguished directly from a gradual process.[17,18]

Under physiologically relevant pH conditions, HX into most proteins occurs in the EX2 limit,[15,19−21] providing a measure of the free energy change associated with a structure-opening reaction (see Supporting Information (SI) text). HX studies have enabled the identification of cooperative units called foldons which are thought to assemble in a sequential manner to form partially unfolded forms (PUFs). Such HX studies have therefore provided an understanding of cooperativity in the context of thermodynamic stability. However, equilibrium data from native state HX experiments do not report on the temporal order of events, and hence, "kinetic cooperativity" can only be addressed by monitoring exchange in the EX1 limit,[22] which provides a measure of structure-opening rates directly.[23−26] In addition, only in the EX1 limit can correlated and uncorrelated opening motions be delineated from the mass distributions seen in HX-MS experiments,[16,27,28] making it possible for a cooperative transition to be distinguished from a continuous transition. Extensive studies[14,29−31] of the refolding and unfolding reactions of the small protein monellin (MNEI), which have revealed that its overall folding reaction is slow, suggest that it is likely to undergo HX in the EX1 limit even under native-like conditions.

In the present work, HX-MS, which probes the solvent exposure of amide backbones all over the protein structure, has been used to describe the degree of cooperativity inherent in the unfolding transition of monellin under native and mildly denaturing conditions. The HX-MS experiments under native-like conditions show that exchange into the protein does indeed occur in the EX1 limit at pH 8. Several amide hydrogens are found to exchange in multiple kinetic phases by uncorrelated local openings. Transient global unfolding, corresponding to the very slow phase of exchange, also occurs via uncorrelated openings in zero denaturant. Stabilization of U by the addition of 0.5 to 1.5 M GdnHCl, or destabilization of N by an increase in pH from 8 to 9, causes transient global unfolding to become a cooperative transition.

## MATERIALS AND METHODS

**Protein Purification.** The method for the purification of MNEI has been described previously.[30] The purity of the protein was confirmed by mass spectrometry. The mass of the protein, as determined from electrospray ionization mass spectrometry (ESI-MS), is 11403 ± 0.3 Da. The protein concentration was determined by measuring the absorbance at 280 nm, using an extinction coefficient of 14 600 $M^{-1}$ $cm^{-1}$.[30]

**Reagents.** All HX reactions were carried out at 25 °C. The reagents used in the experiments were of the highest purity grade from Sigma. Guanidine hydrochloride (GdnHCl) was purchased from USB (USA) and was of the highest purity grade. The labeling buffers, used to initiate the exchange reactions, were 20 mM sodium phosphate at pH 7, 20 mM Tris at pH 8, and 50 mM glycine at pH 9. The quench buffer, used to stop the labeling reaction, was 100 mM glycine hydrochloride, containing 8 M GdnHCl at pH 2.2, on ice. The pH values reported for $D_2O$ buffers are uncorrected for any isotope effect.

**Fluorescence-Monitored Equilibrium and Kinetic Studies.** GdnHCl-induced equilibrium and kinetic unfolding transitions were monitored on the stopped-flow module (SFM4) from Biologic, in the manner described previously.[30] An excitation wavelength of 280 nm was used, and emission was collected at 340 nm using a 10 nm band-pass filter (Asahi Spectra). The final protein concentration was 10 μM.

**Deuteration of MNEI.** MNEI can be fully unfolded at high pH (above 12.5). Exposure of the protein to pH 12.8 for 7−10 min does not result in any significant deamidation or other chemical modification of the protein: the mass of fully protonated protein was found to be altered by less than 0.2 Da by such high pH treatment (data not shown), which is within the error of mass measurement. Hence, the protein was deuterated by unfolding it at pH 12.8 in the presence of $D_2O$ and refolding back at pH 8. The lyophilized protein was dissolved in $D_2O$ buffer (10 mM Tris, pH 8.2), to a final concentration of 200 μM. The pH of the solution was increased to 12.8 by the addition of 1 N NaOD. After 5 min, the pH was dropped to 1.6 by the addition of 1 N DCl and then readjusted slowly to pH 8. The pH was not dropped to 8 directly since the pI of the protein is 8.6 and refolding at pH 8, at high protein concentration, led to the precipitation of the protein. The increase in mass due to deuteration was the same when the protein was heated to 70 °C, in the presence of $D_2O$, for 10 min. However, at higher concentrations, MNEI precipitates upon heating, and the pH jump method was therefore used to deuterate the protein. CD spectra and fluorescence-measured unfolding rates confirmed that the pH jumps did not affect the structure of the protein significantly (data not shown).

**Hydrogen Exchange Kinetics of the Intact Protein.** Seven microliters of deuterated protein (~200 μM concentration) in $D_2O$ buffer (10 mM Tris, pH 8) were diluted 20-fold into 133 μL of exchange buffer (20 mM Tris in $H_2O$, pH 8) to initiate the exchange reaction. After different times of exchange at 25 °C, the reactions were quenched by the addition of 125 μL of the exchange reaction to 375 μL of the quench buffer, on ice. The final quenched reaction contained 2.5 μM protein, 75 mM glycine-HCl (in $H_2O$), and 6 M GdnHCl, at pH 2.6 on ice. The samples were incubated under quenched conditions in 6 M GdnHCl for 1 min to facilitate subsequent fragmentation (see below). For exchange in higher GdnHCl concentrations (0.5−1.5 M GdnHCl), the denaturant concentrations in the exchange and quench buffers were adjusted accordingly.

**Sample Preparation for Electron Transfer Dissociation (ETD).** Segment-specific HX data were obtained by chemical fragmentation of the intact protein after exchange in protonated solvent. Ten microliters of deuterated protein (~500 μM) were diluted 15-fold into 140 μL of exchange buffer to initiate the reaction. The higher protein concentration as well as partial unfolding due to incubation in 6 M GdnHCl provided better ion counts of the fragments obtained from ETD.

**Processing of Samples for Mass Spectrometry.** After incubation in 6 M GdnHCl for 1 min, the quenched reaction was desalted using a Sephadex G-25 Hi-trap column from GE, equilibrated with Milli-Q water, pH 2.6 (pH adjusted with HCl) on ice, in conjunction with an ÄKTA basic HPLC system. To measure the mass of a completely deuterated protein sample, the deuterated protein was desalted with a ZipTip


DOI: 10.1021/acs.biochem.5b00247
Biochemistry 2015, 54, 3431−3441

column and eluted out in 50 μL solvent (50% acetonitrile in $D_2O$). After addition of 145 μL of $D_2O$ and 2 μL of 5% formic acid, the sample was injected directly into the mass spectrometer using a syringe pump.

**Data Acquisition by ESI-MS.** The desalted samples were injected into the HDX module (Waters Corp.) coupled with a nanoACQUITY UPLC system and the Synapt G2 HD mass spectrometer. The protein was loaded onto a C18 reverse phase trap column in 0.05% formic acid at a flow rate of 100 μL/min for 1 min and eluted using a gradient of 35−95% acetonitrile (0.1% formic acid), at a flow rate of 40 μL/min, in 3 min. The chromatography was carried out at 4 °C in the Waters HDX cooling module.

The capillary voltage was set to 3 kV, the source temperature to 80 °C, and the desolvation temperature to 200 °C. A scan duration of 0.5 s was used, and the first 40 scans, from the time at which the protein started eluting, were combined to get a cumulative ion count of ∼$10^6$ for each sample. Between two successive sample runs, 2−3 wash runs were given by injecting Milli-Q water to ensure minimal carryover from the previous runs. The instrument parameters used for ETD fragmentation have been detailed in the SI methods. The combined spectra were background subtracted and smoothened using the MassLynx 4.1 software. The list spectrum option was used to export data to SigmaPlot and Origin.

**Data Analysis.** *(A) Analysis of Hydrogen Exchange Kinetics for the Intact Protein.* The $m/z$ peak having the highest intensity (the 13 charged state) was analyzed at each time point and plotted after normalizing to the area under the peak determined using the Origin software. Further analysis of kinetic rates was done using the SigmaPlot v10 software. The number of deuteriums retained, determined as the difference in the mass of the exchanged sample at each time point and the completely protonated protein, plotted as a function of time were fit to a sum of three exponentials for 0 M GdnHCl and to a sum of two exponentials for higher GdnHCl concentrations. For HX in the presence of 0.5−1.5 M GdnHCl, the fraction of unfolded protein was determined as the area under the peak centered at an $m/z$ of 878.4 ± 0.06 relative to the total area under the 13 charged state peak. The areas and widths were obtained by fitting the $m/z$ distribution to a sum of two Gaussians using the Origin software.

*(B) Analysis of Hydrogen Exchange Kinetics for ETD Fragments.* The $c$ and $z$ ions obtained from chemical fragmentation were identified from the centroid spectra using the BioLynx software. The average mass of each fragment was determined, from the intensity-weighted isotopic abundances, with and without exchange. The deuteriums retained in each $c$ or $z$ ion were determined from the difference in the masses of the fragments obtained from a deuterated and a protonated sample. The deuterium retention of different segments in the protein was obtained by subtracting the deuterium retention of consecutive $c$ and $z$ ions. For example, subtraction of the number of deuteriums retained in the c4 ion (residues 1−5) from those in the c39 ion (residues 1−40) yields the number of deuteriums retained in the protein fragment extending from residues 6 to 40.

*(C) Global Fitting.* The mass spectra, obtained from HX in the absence and presence (1 M) of GdnHCl, at all time points, were globally fit using the MATLAB software to determine the kinetic mechanism of unfolding under native-like conditions. The $m/z$ distribution for the 13 charged state was simulated as described in the SI methods and fitted to the data using *lsqcurvefit*.

## RESULTS

**Hydrogen Exchange under Native Conditions.** Deuterated protein was diluted 20-fold into protonated exchange buffer at pH 8 not containing GdnHCl, and the mass distributions were measured at different times of exchange. The mass of N, determined from the spectrum obtained at 5 s of exchange (Figure 2A), indicated that it retains 44 ± 1

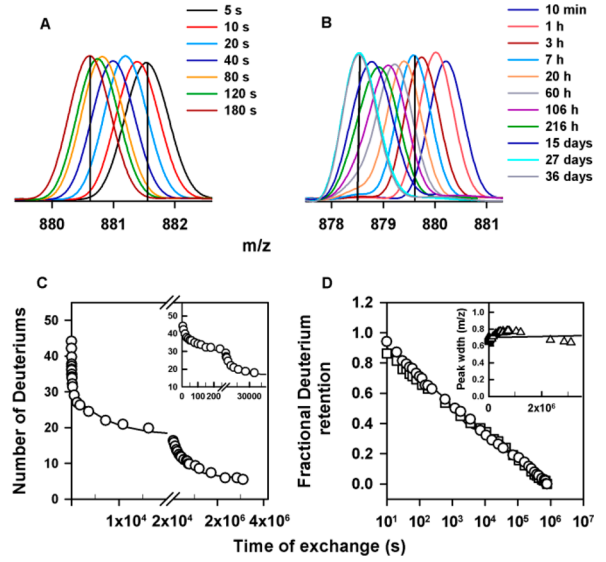


**Figure 2.** Hydrogen exchange in 0 M GdnHCl. Representative spectra (13 charged state) are shown for exchange in 0 M GdnHCl, at pH 8 (A) in the first 3 min, and (B) from 10 min to 36 days. The solid vertical lines represent the centroid $m/z$ values for the N state (5 s), U state (36 days), and for the species populated at the end of each kinetic phase of exchange (see panel C). (C) A plot of the number of deuteriums retained as a function of time of exchange/unfolding fits to the sum of three exponentials which yields the rate constants and amplitudes for the fast and slow phases, as reported in the legend of Figure 4, and of the very slow phase ((1.4 ± 0.007) × $10^{-6}$ $s^{-1}$). The inset shows the data for the first 8 h, corresponding to the fast and slow phases. (D) The fractional deuterium retention measured in 0 M GdnHCl, at pH 7 (□) and pH 8 (○) until 200 h was globally fit (solid line) to a sum of three exponentials to obtain the rate constants for the fast ((2.7 ± 0.7) × $10^{-2}$ $s^{-1}$), slow ((5.1 ± 0.1) × $10^{-4}$ $s^{-1}$), and the very slow ((2.1 ± 0.2) × $10^{-6}$ $s^{-1}$) phases of exchange. The inset shows the width (full width at half-maximum) of the mass distributions at all times of exchange in 0 M GdnHCl at pH 8. The solid line through the data has been drawn to guide the eye.

deuteriums. Only these 44 backbone deuteriums serve as structural probes because all other deuteriums exchange out very rapidly in protonated solvent. In native conditions, at pH 8, it is observed that the mass distribution remains unimodal (Figure 2A,B), for all times until the exchange reaction is complete (36 days), with a constant width (Figure 2D, inset) and shifts only in the centroid value. The variation in the width of the distribution corresponds to a change of 1.7 Da, which is within the range expected for width changes due to isotope incorporations into the protein.[32] A plot of the number of deuteriums retained versus the time of exchange fits well to the sum of three exponentials (Figure 2C), indicating that there are three kinetic phases of HX in 0 M GdnHCl: fast and slow phases which are complete within 3 min and 8 h, respectively,


DOI: 10.1021/acs.biochem.5b00247
*Biochemistry* 2015, 54, 3431−3441

and a very slow phase which is completed in 36 days. At the end of the very slow phase, the protein was found to retain 5 ± 1 deuteriums, which was expected since the exchange was carried out in 95% $H_2O$, 5% $D_2O$. Given the slow rates of exchange, it was important to confirm that the protein is not affected by prolonged incubation in solution, under the experimental conditions used. Figure S1 shows that the protein stability does not change significantly.

**Mechanism of Exchange in 0 M GdnHCl.** In HX-MS experiments, it is very important to distinguish between the EX1 and the EX2 limits of exchange in order to differentiate between cooperative and noncooperative opening motions (see Discussion). The most definitive way to do this is to measure the pH dependence of the observed rates: in the EX1 limit, $k_{obs}$ is independent of pH (eq S2), while in the EX2 limit $k_{obs}$ is proportional to $k_{int}$ and increases 10-fold for every unit increase in pH (eq S3). In 0 M GdnHCl, at pH 7, as at pH 8, unimodal mass spectra are observed to evolve in three observable kinetic phases (Figure S2A,B). The exchange processes at pH 7 and 8 are compared in Figure 2D, in which the deuterium retention was normalized[33] to the total amplitude to account for the fact that the N state retains more deuteriums at pH 7 than at pH 8. The rate constants of the three phases were found to be comparable across pH 7 and pH 8; consequently, the data at both the pH values could be fit globally. The observation that the rate constants of all three kinetic phases of exchange are identical at pH 7 and 8 indicates that the HX in all three kinetic phases takes place in the EX1 limit in 0 M GdnHCl at pH 8. It should be noted that the global stability of MNEI is similar at pH 7 and pH 8, and only slightly lower at pH 9 (Figure S3A), and that the global unfolding rates are similar at the three pH values (Figure S3B).

**Hydrogen Exchange in the Presence of Denaturant.** The exchange kinetics was monitored in the presence of denaturant, at pH 8, by diluting the native, deuterated protein into protonated exchange buffer to have the final desired denaturant concentration (Figures 3 and S4). The mass distribution of N (obtained at 5 s of exchange) in the presence of 1 M GdnHCl is similar to that in the absence of denaturant and continues to shift as a unimodal peak to lower $m/z$ values for the first 3 min of exchange (Figure 3A). At longer exchange times (10 min onward), the distribution becomes bimodal, and two well separated peaks can be observed (Figure 3B). The distribution centered at the lower $m/z$ value corresponds to that for a species with deuterium retention of 4 ± 1, which can be attributed to the 5% deuterium remaining in solution during exchange, suggesting that it represents U that forms transiently. The shift in the centroid $m/z$ value of the higher mass distribution, which corresponds to the loss of the first 25 deuteriums via uncorrelated opening events, takes place in two kinetic phases in the presence of 1 M GdnHCl (Figure 3C), as well as 0.5 and 1.5 M GdnHCl (Figure S4), which correspond to the fast and the slow phases observed in the absence of GdnHCl. The separation between the two peaks of the bimodal distribution at the end of the slow phase corresponds to a mass difference of 14 deuteriums; these slowest exchanging deuteriums become exposed to exchange in a correlated opening motion leading to the formation of the globally unfolded state, which forms transiently in the very slow phase. The time evolution of the fractional area under the peak corresponding to U fits well to a single exponential equation (Figure 3D) and provides a measure of the apparent rate constant of the very slow phase of exchange, which corresponds

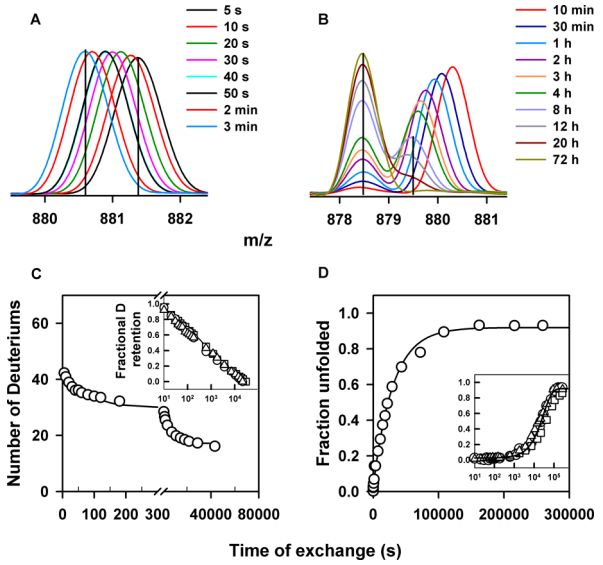


**Figure 3.** Hydrogen exchange in 1 M GdnHCl. Representative spectra are shown for exchange in 1 M GdnHCl, at pH 8 (A) in the first 3 min and (B) from 10 min to 72 h. The solid vertical lines in panels A and B represent the centroid $m/z$ values for the N state (5 s), U state (72 h), and the species populated at the end of each kinetic phase (see panel C). (C) The number of deuteriums retained as a function of time fits to a sum of two exponentials, corresponding to the fast and slow phases, with rate constants and amplitudes as reported in the legend of Figure 4. The inset shows the change in the fractional deuterium retention with time at pH 7 (□), pH 8 (○), and pH 9 (Δ), until 8 h, which was globally fit to a sum of two exponentials to obtain the rate constants of the fast ($(1.1 \pm 0.07) \times 10^{-2}$ $s^{-1}$) and the slow ($(3 \pm 1.6) \times 10^{-4}$ $s^{-1}$) phases of exchange. (D) The increase in the fraction of unfolded species with time fits to a single exponential equation, which yields the rate of the very slow phase ($(3.6 \pm 0.8) \times 10^{-5}$ $s^{-1}$). The inset shows a comparison of the increase in the fraction unfolded with time at pH 7 (□), pH 8 (○), and pH 9 (Δ) which can be globally fit to yield the rate constant of the very slow phase ($(3.2 \pm 0.4) \times 10^{-5}$ $s^{-1}$).

to transient global unfolding of the protein. Hence, like in native-like conditions, exchange in 1 M GdnHCl also proceeds in three kinetic phases. However, unlike in the absence of denaturant, the mass distributions become bimodal in denaturant. The last 14 deuteriums exchange out in a cooperative opening motion in the presence of not only 1 M GdnHCl (Figure 3) but also 0.5 and 1.5 M GdnHCl (Figure S4) in the very slow phase of exchange.

The mechanism of exchange was also determined in the presence of denaturant by measuring $k_{obs}$ at pH 7 (Figure S2C,D) and pH 9 (Figure S5). In 1 M GdnHCl, the three observable kinetic phases overlap in the pH range 7−9 (Figure 3C,D, insets) and can be fit globally. This suggests that in the presence of GdnHCl, exchange in all the three phases takes place in the EX1 limit. The bimodal distribution seen in the very slow phase of exchange (Figure 3B) further supports the result that exchange in the very slow phase proceeds in the EX1 limit.[27]

**Denaturant Dependence of Exchange Rates.** An increase in denaturant concentration does not affect the rates of the fast and the slow phases of exchange significantly (Figure 4A,B). However, the rate of the very slow phase of exchange increases with denaturant (Figure 4C). This is not unexpected since global unfolding leads to an increase in the accessible surface area of the protein, which results in the denaturant


DOI: 10.1021/acs.biochem.5b00247
Biochemistry 2015, 54, 3431−3441

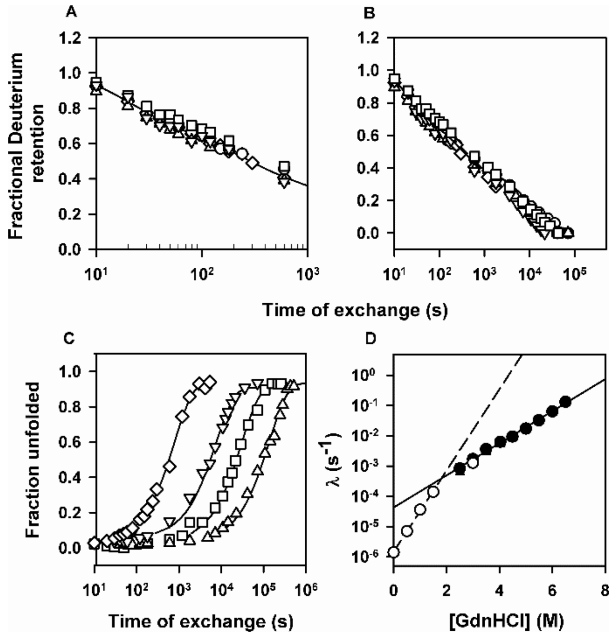


**Figure 4.** Denaturant dependence of hydrogen exchange kinetics at pH 8, 25 °C. The kinetics of the (A) fast, (B) slow, and (C) very slow phases of exchange have been measured as described in the legends to Figures 1 and 2, in 0 M (○), 0.5 M (Δ), 1 M (□), 1.5 M (▼) and 3 M (◊) GdnHCl. The rate constants of the fast and slow phases, determined by globally fitting the kinetic curves in panels A and B to single exponential equations are $(1 \pm 0.5) \times 10^{-2}$ $s^{-1}$ and $(1.4 \pm 0.5) \times 10^{-4}$ $s^{-1}$, respectively. The amplitudes of the fast and slow phases are $13 \pm 1$ and $12 \pm 1$ deuteriums, respectively. The solid lines through the data represent the fits. (D) The apparent rate constant of the very slow phase of hydrogen exchange (○), obtained from a single exponential fit of the fraction unfolded plots in panel C, have been compared to the observed global unfolding rates determined from fluorescence measurements (●). The solid line through the fluorescence data and the dashed line through the HX data are linear regression fits. The error bars, which represent the spreads in the measurements from two separate experiments, are smaller than the size of the symbols.

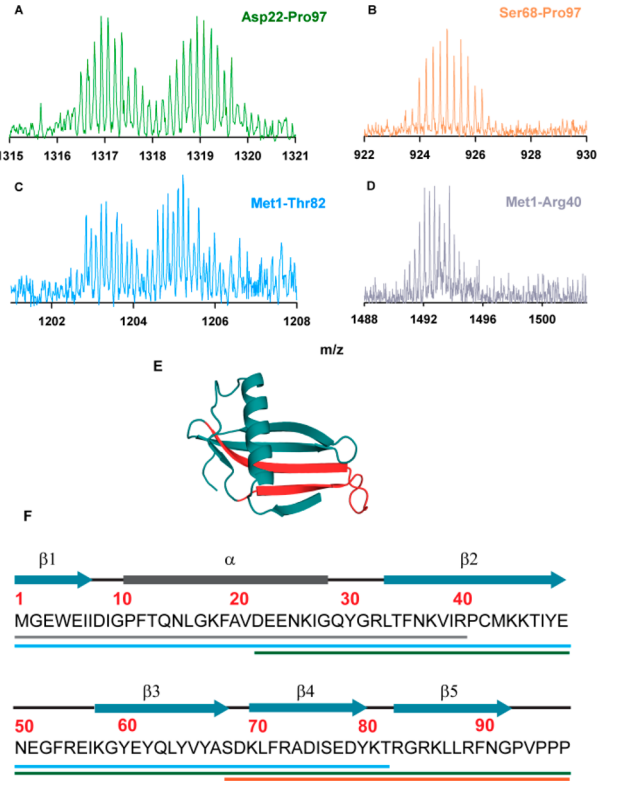


**Figure 5.** Identification of the backbone amide hydrogens which exchange cooperatively. The spectra obtained after 6 h of exchange in 1 M GdnHCl, pH 8 for the sequence stretch (A) Asp22-Pro97, (B) Ser68-Pro97, (C) Met1-Thr82, and (D) Met1-Arg40. (E) The structure of MNEI (PDB ID: 1IV7) with the cooperative unit consisting of the sequence stretch Pro41-Ala67 in $\beta$-strands 2 and 3 highlighted in red. (F) The peptide map of the protein with the ETD fragments shown in color-coded bars below the sequence. The cyan arrows and gray bar above the amino acid sequence indicate the $\beta$-strands and $\alpha$-helix, respectively.

dependence of the rate (see Discussion). A comparison of the rate constant of the very slow phase of exchange in 0.5−1.5 M GdnHCl to global unfolding rates measured by fluorescence in 2−6 M GdnHCl reveals a downward kink in the unfolding arm of the chevron at low denaturant concentrations (Figure 4D).

**Structural Identification of the Cooperative Unit.** In order to identify the amide sites that are involved in the cooperative opening motion in the presence of denaturant, fragments of the protein were analyzed by mass spectrometry, subsequent to HX in 1 M GdnHCl. While most HX-MS studies rely on proteolysis for fragmentation,[34] MNEI was found to be resistant to digestion by pepsin and other acid proteases. Chemical fragmentation by ETD provides an alternative method of fragmenting the protein while causing minimal hydrogen scrambling.[35] Figure 5A,B shows that while the mass distribution of the Asp22-Pro97 sequence stretch becomes bimodal at 6 h of exchange in 1 M GdnHCl, that of the Ser68-Pro97 stretch remains unimodal at all times of exchange (data not shown), indicating that the cooperative unit is localized between the residues Asp22 and Ser68. Similarly, it is evident from Figure 5C,D that the sequence stretch flanked by Arg40 and Thr82 also shows cooperative behavior in the presence of denaturant. All other fragments obtained from ETD showed unimodal mass distributions at all times of exchange (data not shown). Taken together, these data identify the location of the cooperative unit as the sequence stretch between Pro41 and Ala67 (Figure 5E).

The difference in mass between the two peaks seen for the Asp22-Pro97 segment as well as for the Met1-Thr82 segment, is 14 Da, which corresponds to the size of the cooperative unit observed for the intact protein, under the same conditions (Figure 3B). This suggests that the only part of MNEI that exchanges cooperatively in the presence of denaturant resides in the Pro41-Ala67 sequence stretch, spanning two adjacent $\beta$-strands. In the absence of denaturant, the 14 deuteriums in the Pro41-Ala67 sequence stretch exchange out in an uncorrelated manner like all other deuteriums.

**Exchange at pH 9.** Figure 6A,B shows representative spectra for exchange in 0 M GdnHCl, at pH 9. A unimodal mass distribution shifts to lower $m/z$ with increasing time of exchange in three kinetic phases (Figure 6C). From 7 h onward, peak widening is observed and the mass distributions can be fit to a sum of two Gaussian distributions (Figure 6B), with the lower $m/z$ peak corresponding in mass to that of the U state. The separation between the two peaks of the bimodal mass distribution suggests that seven deuteriums exchange out in the slowest phase of exchange. The fractional area under the lower mass peak was used to determine the rate at which the



DOI: 10.1021/acs.biochem.5b00247
*Biochemistry* 2015, 54, 3431−3441

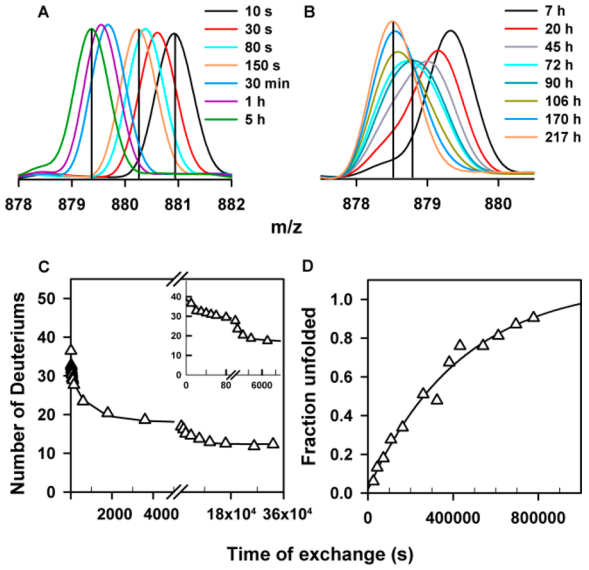


**Figure 6.** Hydrogen exchange in 0 M GdnHCl, at pH 9, 25 °C. Representative spectra are shown for exchange in (A) the first 5 h and (B) from 7 to 217 h. The solid vertical lines in panels A and B represent the centroid $m/z$ values for the N state (5 s) and the species populated at the end of each kinetic phase (see panel C). (C) The number of deuteriums retained as a function of time of exchange, up to 90 h, fits to a sum of three exponentials corresponding to the rate constants $(2.8 \pm 0.2) \times 10^{-2}$ $s^{-1}$, $(1.2 \pm 0.2) \times 10^{-4}$ $s^{-1}$, and $(2.4 \pm 0.6) \times 10^{-5}$ $s^{-1}$. The inset shows an expanded view of the first two phases. (D) The increase in the fraction of unfolded molecules fits to a single exponential equation with an apparent rate constant of $(2.25 \pm 0.07) \times 10^{-6}$ $s^{-1}$.

unfolded state is transiently formed, in the slowest phase of exchange (Figure 6D). The most striking difference between native-state exchange at pH 9 and at lower pH (7 and 8) is that at pH 9 the mass distributions widen in the slowest phase of exchange. This suggests an increase in the cooperativity of the global unfolding transition upon an increase in the pH, similar to that observed upon the addition of denaturant, albeit with a smaller cooperative unit consisting of around seven deuteriums at the higher pH.

Exchange in the presence of 1 M GdnHCl at pH 9 is very similar to that in 1 M GdnHCl at pH 8 and pH 7. There are three observable kinetic phases of exchange (Figure 3C–D insets), and the mass distributions evolve in a bimodal manner (Figure S5) during the very slow phase of exchange. The separation between the two peaks of the bimodal mass distribution suggests that 11 deuteriums exchange out in the very slow phase of exchange. The presence of two distinct and well separated mass distributions in 1 M GdnHCl at pH 9 further indicates that the size of the cooperative unit, involved in the global unfolding transition in 0 M GdnHCl at pH 9, increases upon the addition of denaturant.

## DISCUSSION

The focus of the present study is to understand the origin of the cooperativity inherent in the unfolding transition of a protein and the factors that modulate it. The HX-MS experiments have allowed a delineation of the ruggedness of the free energy surface of the protein MNEI under native-like conditions. Changes in solvent conditions that affect the stabilities of N and U are found to modulate the energy landscape and affect the cooperativity of structure-opening transitions in the protein.

**Hydrogen Exchange Takes Place in the EX1 Limit.** The mass distributions obtained in HX-MS spectra provide a measure of the population distributions, which can directly distinguish between cooperative and noncooperative transitions.[16,27,28,36] Exchange itself is correlated in the EX1 limit (SI text), and every opening event leads to exchange. Hence, correlated and cooperative opening of multiple amide sites, followed by correlated exchange in the EX1 limit, leads to bimodal spectra in which one peak corresponds to the exchanged and the other to the unexchanged species.[27,28,36] On the other hand, uncorrelated and noncooperative opening events followed by exchange in the EX1 limit result in unimodal spectra, corresponding to the exchange of one or two deuteriums at a time. In the EX2 limit (SI text), a certain amide site may open and close several times prior to exchange. Uncorrelated exchange in the EX2 limit therefore leads to unimodal mass distributions, irrespective of whether the opening motions are correlated or uncorrelated.[16,27] Hence cooperative and noncooperative openings can be distinguished from mass distributions describing HX only in the EX1 limit. But mass spectra resulting from uncorrelated motions followed by exchange in the EX1 limit would be similar to those observed in the EX2 limit. Hence, in order to distinguish between correlated and uncorrelated transitions, it is very important to establish that exchange does indeed take place in the EX1 limit. For MNEI, a lack of pH dependence of the observed exchange rates, for all kinetic phases, in the absence (Figure 2D) and in the presence (Figure 3C,D, insets) of denaturant confirms that exchange at pH 8 takes place in the EX1 limit. The unimodal mass spectra observed for MNEI are therefore indicative of uncorrelated opening motions, and not of exchange in the EX2 limit, while bimodal distributions suggest cooperative opening processes.

**Evidence for Multiple Opening Reactions.** Exchange in the EX1 limit also allows a direct determination of the opening rates for backbone amides (SI text). The fast and slow kinetic phases of exchange therefore correspond to multiple opening reactions which occur over widely dispersed time scales (Figures 2C and 3C), in the presence and absence of denaturant. The continuous shift in the mass distributions in both phases, in 0 M (Figure 2A,B) and in 1 M GdnHCl (Figure 3A,B), as well as in 0.5 and 1.5 M GdnHCl (Figure S4), with no significant changes in width, further indicates that the first 25 deuteriums are lost via uncorrelated opening events. Both phases are orders of magnitude faster than the global unfolding rates, expected from fluorescence measurements (Figure 4D), suggesting that these opening events lead to the sampling of two partially unfolded forms, $I_1$ and $I_2$, on the native side of the major unfolding barrier. The lack of denaturant dependence of the fast and slow rates (Figure 4A,B) indicates that there is no appreciable change in surface area upon unfolding to $I_1$ and $I_2$. This is consistent with 1–2 deuteriums at a time becoming exposed to exchange in multiple uncorrelated steps. Uncorrelated openings in the EX1 limit, and a lack of denaturant dependence, are typically interpreted as local fluctuations.[28,33,37] However, in this case the multiexponential kinetics strongly suggests that partially unfolded forms are sampled at the end of the fast and slow kinetic phases of exchange. The relatively slow rates of the fast and slow phases as well as the wide dispersion in the time scales further indicate that the uncorrelated openings which result in the transient formation


DOI: 10.1021/acs.biochem.5b00247
Biochemistry 2015, 54, 3431–3441

of $I_1$ and $I_2$ are associated with specific structural transitions in the protein (see below).

**Global Unfolding in the Absence and Presence of Denaturant.** In the absence of denaturant, the slowest exchanging deuteriums open via uncorrelated motions resulting in unimodal mass distributions (Figure 2A,B). This has been observed to date only in the case of the turkey ovomucoid third domain, in which the slowest exchanging sites open by uncorrelated motions, leading to global unfolding.[23,24] But very interestingly in the case of MNEI, the addition of low concentrations of denaturant (0.5 M GdnHCl and above) causes the spectra to become bimodal (Figures 3 and S4), and the last 14 deuteriums open in a correlated manner, indicating an increase in cooperativity in the presence of denaturant.

For most proteins, the opening of the slowest exchanging deuteriums has been observed to correspond to the global unfolding transition, in terms of $\Delta G_{HX}$, the free energy change associated with the opening[15,38−40] as well as the rate of opening.[41,42] In the case of MNEI, the rate of the very slow phase of exchange at low GdnHCl concentrations is slower than the rate of global unfolding expected from extrapolation of fluorescence-measured unfolding rates to low GdnHCl concentrations (Figure 4D). It should be noted here that global unfolding rates at such low GdnHCl concentrations cannot be ascertained by fluorescence measurements because a very small percentage of the protein molecules are unfolded at equilibrium under the native-like conditions used. The denaturant-dependence of the apparent rate constant of very slow exchange, at zero and low GdnHCl concentrations, merges into the denaturant-dependence of the apparent rate constants of global unfolding at high GdnHCl concentrations, although a sharp kink is observed in the overall dependence on GdnHCl concentration. In the case of other proteins for which unfolding rates measured by HX were found to be slower than extrapolated global unfolding rates and for which kinks in the denaturant dependences were similarly observed,[12,43] the observations could be attributed to the population of an on-pathway unfolding intermediate (see below). The observation that at 3 M GdnHCl the rates measured by HX and fluorescence are the same suggests that the rate constant of very slow transient structural opening measured by HX at low GdnHCl concentrations corresponds to a rate constant of global unfolding. It is remarkable that the mean waiting time for all of the amide deuteriums in the protein to exchange out through transient structural opening events corresponds to the mean waiting time for the protein to unfold completely. This suggests that the transient structure-opening fluctuations that enable HX are the same fluctuations that lead to global unfolding of the protein.

An important factor to be considered in all HX experiments is that local motions that expose backbone amides to exchange may obscure the observation of actual structure-opening events. In the EX2 limit of exchange, local fluctuations are typically identified by the low values as well as a lack of denaturant dependence of $\Delta G_{HX}$.[15] In the EX1 limit, while structural transitions are inferred usually from correlated openings which expose multiple amides at a time, uncorrelated exchange is typically interpreted as local fluctuations.[28,33,37] The strongest evidence suggesting that the uncorrelated opening events in MNEI in the absence of denaturant are associated with structure-opening events is the observation of three kinetic phases of exchange which are orders of magnitude different from each other in rates. This indicates that there are at least three classes of backbone amides in the protein, with three different mean waiting times of exchange, which are more likely to correspond to different structural transitions than to local fluctuations which should ideally have similar waiting times, when not limited by structure. It has been observed in previous HX studies that even if local motion exposes only one site at a time, it can be associated with structural changes that affect several neighboring residues.[44]

The significant denaturant dependence of the very slow phase of exchange (Figure 4D) further indicates that the protein undergoes a considerable change in exposed surface area in this phase. The depth of the backbone amides in MNEI varies from 3.3 Å for amides on the surface of the protein, to 8.45 Å for deeply buried amides. Given that complete exchange has occurred at the end of the very slow phase observed in 0 M GdnHCl, it is very unlikely that such deeply buried amides exchange by local motions which are not limited by the structure of the protein. These observations therefore make it very likely that, although the backbone amides open one at a time during the very slow phase of exchange in the absence of denaturant, the very slow phase results in the transient formation of the globally unfolded state. Upon the addition of denaturant, the very slow phase of exchange manifests itself in a bimodal mass distribution, and the 14 slowest exchanging deuteriums that exchange out individually in an uncorrelated manner in the absence of denaturant now exchange out together in a correlated manner. Hence the $\beta$-sheet structure encompassed by the sequence stretch between Pro41 and Ala67 (Figure 5E) appears to unfold noncooperatively in the absence of denaturant but cooperatively in the presence of denaturant.

**Tuning the Cooperativity of the Global Unfolding Transition.** Under native conditions the U state is extremely unstable, and hence, insignificantly populated. The global unfolding reaction appears to be a one-state, uphill, gradual transition (Figure 2). Upon the addition of denaturant, the unfolding transition becomes barrier-limited and therefore cooperative (Figure 3). The possible explanations for the observed switch in cooperativity are that either the U state is stabilized or the N state is destabilized upon the addition of denaturant (Figure 1). There is debate in the literature about the mode of action of chemical denaturants.[26,45−48] A denaturant has a preferential free energy of interaction with the U state with respect to the N state because the U state has more surface area exposed for the denaturant to bind to, than does the N state.[47,49−51] The higher extent of binding to (association of) the denaturant with the U state can be expected to lower the free energy of the U state with respect to the N state.

Upon addition of denaturant, unfolding is accelerated (Figure 4D), indicating that the transition state becomes stabilized with respect to the N state. The addition of denaturant also decelerates folding,[30] indicating that the transition state becomes destabilized with respect to the U state. Hence upon addition of denaturant, the transition state must be stabilized less than the U state, with respect to the N state. Since the transition state will have less surface area exposed than does the U state, it is expected to be stabilized less than the U state, with respect to the N state. This is an important point: it is evident from Figure 1 that a barrierless transition would switch to a barrier-limited process only if the U state is stabilized more than the transition state with respect to the N state, upon the addition of denaturant. This difference



DOI: 10.1021/acs.biochem.5b00247
*Biochemistry* 2015, 54, 3431−3441

in relative stabilization therefore leads to the presence of a free energy barrier that did not exist under strongly folding conditions (zero denaturant), resulting in two-state-like behavior. It is remarkable that conditions that are typically used to decrease the stability of a protein (such as an increase in denaturant concentration), and to measure the cooperativity of the unfolding reaction, are themselves responsible for making the transition more cooperative.[52]

The Pro41-Ala67 sequence stretch, which spans two $\beta$-strands, constitutes the cooperative unfolding unit in the presence of denaturant. All 14 deuteriums observed to exchange in this stretch open via a correlated motion in the presence of GdnHCl, but exchange gradually in 0 M GdnHCl. The backbone amides in the Pro41-Ala67 stretch are some of the most deeply buried in the protein and also have the slowest rates of exchange, suggesting that this segment is one of the most stable parts of MNEI and is a part of the core of the protein. It is expected that the barrier induced in the presence of denaturant would affect the slowest structural transition during unfolding.

**Global Unfolding at Higher pH.** It is evident from Figure 1 that a transition from a one-state to a two-state process can be effected not only by stabilization of U but also by destabilization of N. The stability of MNEI decreases by 1 kcal mol$^{-1}$, with an increase in pH from 8 to 9 (Figure S3), which has been attributed to a decrease in the stability of N due to the deprotonation of a buried cysteine residue in the protein.[53] The addition of 0.5 M GdnHCl, which is the lowest denaturant concentration at which a cooperative global unfolding transition has been observed in this study, causes a similar change in stability. A comparison of the exchange kinetics at pH 8 and 9 should therefore allow a better understanding of how experimental conditions can modulate the cooperativity of the global unfolding transition in MNEI. In the absence of denaturant, at pH 9 (Figure 6), bimodality can be inferred from a widening of the mass distributions in the slowest phase of exchange. The observation of peak widening, and the absence of two distinct mass distributions, suggest that fewer sites undergo correlated opening, and that the size of the cooperative unit for unfolding at pH 9, 0 M GdnHCl is smaller than that for unfolding at pH 8, 1 M GdnHCl. At pH 9, the addition of denaturant, increases the size of the structural unit undergoing cooperative transitions, indicated by the observation of well separated peaks (Figure S5).

Thus, while an increase in pH alone from pH 8 to 9 in the absence of denaturant also causes an increase in the cooperativity of unfolding, the size of the cooperative unit is smaller (seven deuteriums exchange cooperatively) than that observed upon an increase in denaturant alone from 0 to 1 M GdnHCl, either at pH 8 (14 deuteriums exchange cooperatively) or at pH 9 (11 deuteriums exchange cooperatively). This indicates that the degree of cooperativity induced by the increase in pH is less than that induced by the addition of GdnHCl. It is evident that experimental conditions which modulate the stabilities of the N and U states to result in similar free energy differences between N and U induce different degrees of cooperativity because of different effects on the structure of the protein.

**Kinetic Mechanism of Unfolding under Native-Like Conditions.** In order to describe a kinetic mechanism that incorporates the N and the U states, as well as the partially unfolded forms $I_1$ and $I_2$, the mass spectra at all times of exchange in 0 and 1 M GdnHCl were fit globally using a MATLAB program, according to both sequential and off-pathway schemes as described in the SI methods. It should be noted that the HX data do not explicitly show that $I_1$ and $I_2$ are sampled sequentially in the course of the protein sampling U but show only that the intermediates are sampled on faster time scales than is U. Although a sequential scheme (Scheme S2) was found to be the simplest mechanism which provides satisfactory fits to the mass spectra describing HX in 0 and 1 M GdnHCl, the possibility of an off-pathway mechanism cannot be eliminated on the basis of the fits alone (see SI text). It is, however, evident that irrespective of the kinetic scheme, N exchanges a significant number of structurally protected deuteriums via multiple opening reactions. While the multi-exponential kinetics reveals the presence of at least two intermediates, the time evolution of the mass distributions shows that the transition to each of the intermediates occurs through a continuum of states.

The logarithm of the unfolding rate constant is expected to have a linear denaturant dependence for a "two-state" process, while deviations from linearity can have multiple implications,[43,54,55] such as a movement of the transition state along a broad energy barrier[56] resulting in a smooth curvature in the unfolding arm. A sharp kink, as observed in the case of MNEI (Figure 4D) is, however, indicative of a change in the rate limiting step of unfolding due to the presence of an on-pathway protected intermediate.[12,43] The shift in the rate-determining step is caused by a change in the stability of the intermediate upon denaturant addition. The on-pathway intermediate cannot, however, be correlated to $I_1$ or $I_2$, at the present time.

**Energy Landscape of Unfolding under Native-Like Conditions.** Native state HX experiments have typically been carried out in the EX2 limit and have provided an understanding of cooperativity in the context of thermodynamic stability. Such studies have identified distinct cooperatively unfolding units in several proteins, including cytochrome $c$[15] and RNaseH,[19] based on discrete $\Delta G_{HX}$ values. For some proteins, such as T4 lysozyme,[57] a continuous dispersion of the $\Delta G_{HX}$ values suggested that the N state was in equilibrium with a multitude of partially unfolded forms. In the case of Staphylococcal nuclease,[58] native state HX data could not distinguish between different partially unfolded forms due to a spread in the $\Delta G_{HX}$ values. All of these previous studies were unable to address the question of kinetic cooperativity under the same experimental conditions because they were carried out in the EX2 limit: they could not temporally resolve the sequence of cooperative unfolding events. Hence, these previous studies carried out in the EX2 limit also could not show that unfolding can switch from being cooperative to being noncooperative upon a change in experimental conditions. Kinetic cooperativity can only be addressed by monitoring exchange in the EX1 limit.[22] In the current study carried out in the EX1 limit of HX, it has been possible not only to establish the temporal sequence of unfolding events but also to demonstrate that the structural transitions during unfolding can occur in a gradual manner and not in a cooperative manner.

The HX data indicate that U, as well as $I_1$ and $I_2$, are sampled through a continuum of structure-opening events. Nevertheless, the overall kinetics of transient opening to $I_1$ and to $I_2$ or to U is exponential in nature. It should be noted that while a barrier-limited process will show exponential kinetics, the observation of exponential kinetics does not necessarily imply that the process being observed is barrier-limited. In fact, barrier-less transitions may also show exponential kinetics.[6,59,60] The most


DOI: 10.1021/acs.biochem.5b00247
Biochemistry 2015, 54, 3431−3441

definitive way to establish the occurrence of a continuous transition is to analyze the population distributions as unfolding proceeds.[17,18] The present work demonstrates that MNEI undergoes gradual transient unfolding under native conditions: the mass distributions obtained from HX-MS reveal that when U is appropriately destabilized, backbone amides lose protection in an entirely noncooperative manner.

In the absence of denaturant at pH 8, MNEI samples the globally unfolded state via noncooperative opening motions which populate a continuum of species between the N and U states (Figure 7). While the multiple kinetic phases indicate the presence of discrete intermediates ($I_1$ and $I_2$), the mass distributions provide evidence of gradual transitions between these states. Thus, the energy landscape of MNEI is extremely rugged in native conditions. Since the HX measurements in 0 M GdnHCl were made under equilibrium conditions, the refolding mechanism should be the reverse of the unfolding mechanism. The multiple pathways and intermediates involved in the refolding of MNEI[30] as well as the relatively slow time scales of refolding further imply that there is considerable roughness in the free energy landscape of this protein.

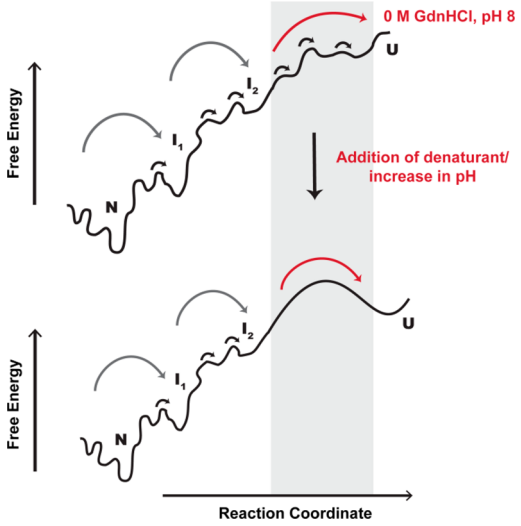


**Figure 7.** Free energy profiles of MNEI under native conditions at pH 8 (upper panel) and upon an increase in denaturant or pH (lower panel). The gray arrows represent the fast and slow kinetic phases which lead to the formation of $I_1$ and $I_2$, respectively, while the small black arrows represent the crossing of smaller barriers which make the landscape rugged. The red arrows correspond to the global unfolding transition (gray shaded region). It should be noted here that although a free energy profile such as this implies a sequential pathway, a kinetic mechanism cannot be assumed.

Under destabilizing conditions, such as upon the addition of denaturant or an increase in pH, a significant barrier to global unfolding is induced due to the stabilization of U or the destabilization of N, respectively (Figure 7). Such a switch has been observed for several fast folding proteins[60−62] which show apparently two-state folding under destabilizing conditions, and which switch to one-state downhill folding when the N state is stabilized by modulating the temperature,[63] solvent conditions, or even the native structure via mutations.[64] Highly denaturing conditions which reduce the activation energy barrier to unfolding may cause a similar switch to a gradual unfolding regime, which has been observed before for MNEI.[18] Theoretical studies with coarse-grained protein models have also been able to capture a switch in cooperativity with stabilization of the unfolded state.[65] The all-or-none exchange of the last 14 deuteriums in the presence of denaturant, compared to the loss of deuteriums one at a time in 0 M GdnHCl, further suggests that several small barriers are smoothened to result in a single activation energy barrier upon the addition of denaturant.

Kinetic evidence for gradual folding transitions has been limited to experimental conditions in which the activation energy barrier was so significantly reduced that folding became an essentially downhill process. The exchange kinetics of MNEI under native conditions demonstrates that even for a very slow unfolding transition, which is limited by a significantly large free energy difference between the N and U states, unfolding can take place through a continuum of states.

## CONCLUSIONS

The present HX-MS study on MNEI sheds light on the nature of the global unfolding transitions that take place under native and mildly denaturing conditions. The mass distributions monitored in the EX1 limit allow uncorrelated openings to be directly distinguished from correlated motions. Under native conditions, MNEI diffuses "uphill" along a rugged free energy surface and samples a continuum of states before sampling the globally unfolded form. Solvent conditions that stabilize the U state, such as an increase in denaturant concentration, result in a cooperative two-state like global unfolding transition over a significant free energy barrier. The increase in cooperativity under conditions that stabilize the U state may have evolved to protect proteins against aggregation. The present study provides direct experimental evidence for a continuum of structure-opening events even in the presence of a large free energy difference between N and U, which slows down unfolding. It also provides an understanding of how the experimental conditions that are typically used to study unfolding transitions in proteins can themselves modulate the energy landscape resulting in the transformation of a gradual process into a cooperative transition.

## ASSOCIATED CONTENT

### Supporting Information

(1) Hydrogen exchange theory, (2) detailed methodology of chemical fragmentation by ETD, (3) detailed description of global fitting. The Supporting Information is available free of charge on the ACS Publications website at DOI: 10.1021/acs.biochem.5b00247.

## AUTHOR INFORMATION

### Corresponding Author

*Fax: 91-80-23636662. E-mail: jayant@ncbs.res.in.

### Funding

J.B.U. is a recipient of a JC Bose National Research Fellowship from the Government of India. This work was funded by the Tata Institute of Fundamental Research and by the Department of Science and Technology, Government of India.

### Notes

The authors declare no competing financial interest.

## ACKNOWLEDGMENTS

We thank Shachi Gosavi, Raghavan Varadarajan, Hue Sun Chan, and members of our laboratory for discussions. We thank Hemanth Giri Rao for help with MATLAB.



DOI: 10.1021/acs.biochem.5b00247
*Biochemistry* 2015, 54, 3431−3441

## ■ ABBREVIATIONS

MNEI, single chain monellin; GdnHCl, guanidine hydrochloride; HX-MS, hydrogen exchange coupled to mass spectrometry; ETD, electron transfer dissociation; PUF, partially unfolded form; $\Delta G_{HX}$, free energy of opening of structure to hydrogen exchange

## ■ REFERENCES


(1) Bryngelson, J. D., Onuchic, J. N., Socci, N. D., and Wolynes, P. G. (1995) Funnels, pathways, and the energy landscape of protein folding: A synthesis. *Proteins Struct. Funct. Bioinforma 21*, 167−195.

(2) Chan, H. S., Zhang, Z., Wallin, S., and Liu, Z. (2011) Cooperativity, local-nonlocal coupling, and nonnative interactions: Principles of protein folding from coarse-grained models. *Annu. Rev. Phys. Chem. 62*, 301−326.

(3) Lakshmikanth, G. S., Sridevi, K., Krishnamoorthy, G., and Udgaonkar, J. B. (2001) Structure is lost incrementally during the unfolding of barstar. *Nat. Struct Mol. Biol. 8*, 799−804.

(4) Li, H., and Frieden, C. (2007) Comparison of C40/82A and P27A C40/82A Barstar Mutants Using 19F NMR. *Biochemistry 46*, 4337−4347.

(5) Rami, B. R., and Udgaonkar, J. B. (2002) Mechanism of Formation of a Productive Molten Globule Form of Barstar. *Biochemistry 41*, 1710−1716.

(6) Sinha, K. K., and Udgaonkar, J. B. (2008) Barrierless evolution of structure during the submillisecond refolding reaction of a small protein. *Proc. Natl. Acad. Sci. U. S. A. 105*, 7998−8003.

(7) Sabelko, J., Ervin, J., and Gruebele, M. (1999) Observation of strange kinetics in protein folding. *Proc. Natl. Acad. Sci. U. S. A. 96*, 6031−6036.

(8) Garcia-Mira, M. M., Sadqi, M., Fischer, N., Sanchez-Ruiz, J. M., and Muñoz, V. (2002) Experimental Identification of Downhill Protein Folding. *Science 298*, 2191−2195.

(9) Frauenfelder, H., Parak, F., and Young, R. D. (1988) Conformational Substates in Proteins. *Annu. Rev. Biophys. Biophys. Chem. 17*, 451−479.

(10) Epstein, D. M., Benkovic, S. J., and Wright, P. E. (1995) Dynamics of the Dihydrofolate Reductase-Folate Complex: Catalytic Sites and Regions Known To Undergo Conformational Change Exhibit Diverse Dynamical Features. *Biochemistry 34*, 11037−11048.

(11) Nardo, A. A. Di, Davidson, A. R., Dobson, C. M., Kay, L. E., Korzhnev, D. M., Salvatella, X., and Vendruscolo, M. (2004) Low-populated folding intermediates of Fyn SH3 characterized by relaxation dispersion NMR. *Nature 430*, 586−590.

(12) Sridevi, K., and Udgaonkar, J. B. (2002) Unfolding rates of barstar determined in native and low denaturant conditions indicate the presence of intermediates. *Biochemistry 41*, 1568−1578.

(13) Bernstein, R., Schmidt, K. L., Harbury, P. B., and Marqusee, S. (2011) Structural and kinetic mapping of side-chain exposure onto the protein energy landscape. *Proc. Natl. Acad. Sci. U. S. A. 108*, 10532−10537.

(14) Malhotra, P., and Udgaonkar, J. B. (2014) High-Energy Intermediates in Protein Unfolding Characterized by Thiol Labeling under Nativelike Conditions. *Biochemistry 53*, 3608−3620.

(15) Bai, Y., Sosnick, T., Mayne, L., and Englander, S. (1995) Protein folding intermediates: native-state hydrogen exchange. *Science*, 192−197.

(16) Miranker, A., Robinson, C. V., Radford, S. E., Aplin, R. T., and Dobson, C. M. (1993) Detection of transient protein folding populations by mass spectrometry. *Science 262*, 896−900.

(17) Chan, H. S., Bromberg, S., and Dill, K. A. (1995) Models of cooperativity in protein folding. *Philos. Trans. R. Soc. London B. Biol. Sci. 348*, 61−70.

(18) Jha, S. K., Dhar, D., Krishnamoorthy, G., and Udgaonkar, J. B. (2009) Continuous dissolution of structure during the unfolding of a small protein. *Proc. Natl. Acad. Sci. U. S. A. 106*, 11113−11118.

(19) Chamberlain, A. K., Handel, T. M., and Marqusee, S. (1996) Detection of rare partially folded molecules in equilibrium with the native conformation of RNaseH. *Nat. Struct. Mol. Biol. 3*, 782−787.

(20) Juneja, J., and Udgaonkar, J. B. (2002) Characterization of the Unfolding of Ribonuclease A by a Pulsed Hydrogen Exchange Study: Evidence for Competing Pathways for Unfolding. *Biochemistry 41*, 2641−2654.

(21) Bhutani, N., and Udgaonkar, J. B. (2003) Folding subdomains of thioredoxin characterized by native-state hydrogen exchange. *Protein Sci. 12*, 1719−1731.

(22) Kaya, H., and Chan, H. S. (2005) Explicit-chain model of native-state hydrogen exchange: Implications for event ordering and cooperativity in protein folding. *Proteins Struct. Funct. Bioinforma. 58*, 31−44.

(23) Arrington, C. B., Teesch, L. M., and Robertson, A. D. (1999) Defining Protein Ensembles with Native-state NH Exchange: Kinetics of Interconversion and Cooperative Units from Combined NMR and MS Analysis. *J. Mol. Biol. 285*, 1265−1275.

(24) Arrington, C. B., and Robertson, A. D. (2000) Correlated motions in native proteins from MS analysis of NH exchange: evidence for a manifold of unfolding reactions in ovomucoid third domain. *J. Mol. Biol. 300*, 221−232.

(25) Hoang, L., Bedard, S., Krishna, M. M. G., Lin, Y., and Englander, S. W. (2002) Cytochrome c folding pathway: kinetic native-state hydrogen exchange. *Proc. Natl. Acad. Sci. U. S. A. 99*, 12173−12178.

(26) Wani, A. H., and Udgaonkar, J. B. (2009) Native state dynamics drive the unfolding of the SH3 domain of PI3 kinase at high denaturant concentration. *Proc. Natl. Acad. Sci. U. S. A. 106*, 20711−20716.

(27) Ferraro, D. M., Lazo, N. D., and Robertson, A. D. (2003) EX1 Hydrogen Exchange and Protein Folding. *Biochemistry 43*, 587−594.

(28) Wales, T. E., and Engen, J. R. (2006) Partial unfolding of diverse SH3 domains on a wide timescale. *J. Mol. Biol. 357*, 1592−1604.

(29) Kimura, T., Uzawa, T., Ishimori, K., Morishima, I., Takahashi, S., Konno, T., Akiyama, S., and Fujisawa, T. (2005) Specific collapse followed by slow hydrogen-bond formation of beta-sheet in the folding of single-chain monellin. *Proc. Natl. Acad. Sci. U. S. A. 102*, 2748−2753.

(30) Patra, A. K., and Udgaonkar, J. B. (2007) Characterization of the folding and unfolding reactions of single-chain monellin: evidence for multiple intermediates and competing pathways. *Biochemistry 46*, 11727−11743.

(31) Jha, S. K., and Udgaonkar, J. B. (2009) Direct evidence for a dry molten globule intermediate during the unfolding of a small protein. *Proc. Natl. Acad. Sci. U. S. A. 106*, 12289−12294.

(32) Weis, D. D., Wales, T. E., Engen, J. R., Hotchko, M., and Ten Eyck, L. F. (2006) Identification and characterization of EX1 kinetics in H/D exchange mass spectrometry by peak width analysis. *J. Am. Soc. Mass Spectrom. 17*, 1498−1509.

(33) Canet, D., Last, A. M., Tito, P., Sunde, M., Spencer, A., Archer, D. B., Redfield, C., Robinson, C. V., and Dobson, C. M. (2002) Local cooperativity in the unfolding of an amyloidogenic variant of human lysozyme. *Nat. Struct. Biol. 9*, 308−315.

(34) Zhang, Z., and Smith, D. L. (1993) Determination of amide hydrogen exchange by mass spectrometry: a new tool for protein structure elucidation. *Protein Sci. 2*, 522−531.

(35) Rand, K. D., Pringle, S. D., Morris, M., Engen, J. R., and Brown, J. M. (2011) ETD in a traveling wave ion guide at tuned Z-spray ion source conditions allows for site-specific hydrogen/deuterium exchange measurements. *J. Am. Soc. Mass Spectrom. 22*, 1784−93.

(36) Wales, T. E., and Engen, J. R. (2006) Hydrogen exchange mass spectrometry for the analysis of protein dynamics. *Mass Spectrom. Rev. 25*, 158−170.

(37) Englander, S. W. (2000) Protein Folding Intermediates and Pathways Studied by Hydrogen Exchange. *Annu. Rev. Biophys. Biomol. Struct. 29*, 213−238.

(38) Kim, K. S., Fuchs, J. A., and Woodward, C. K. (1993) Hydrogen exchange identifies native-state motional domains important in protein folding. *Biochemistry 32*, 9600−9608.




DOI: 10.1021/acs.biochem.5b00247
*Biochemistry* 2015, 54, 3431−3441

(39) Perrett, S., Clarke, J., Hounslow, A. M., and Fersht, A. R. (1995) Relationship between Equilibrium Amide Proton Exchange Behavior and the Folding Pathway of Barnase. *Biochemistry 34*, 9288−9298.
(40) Huyghues-Despointes, B. M. P., Scholtz, J. M., and Pace, C. N. (1999) Protein conformational stabilities can be determined from hydrogen exchange rates. *Nat. Struct Mol. Biol. 6*, 910−912.
(41) Arrington, C. B., and Robertson, A. D. (1997) Microsecond Protein Folding Kinetics from Native-State Hydrogen Exchange. *Biochemistry 36*, 8686−8691.
(42) Sivaraman, T., Arrington, C. B., and Robertson, A. D. (2001) Kinetics of unfolding and folding from amide hydrogen exchange in native ubiquitin. *Nat. Struct Mol. Biol. 8*, 331−333.
(43) Fersht, A. R. (2000) A kinetically significant intermediate in the folding of barnase. *Proc. Natl. Acad. Sci. U. S. A. 97*, 14121−14126.
(44) Maity, H., Lim, W. K., Rumbley, J. N., and Englander, S. W. (2003) Protein hydrogen exchange mechanism: Local fluctuations. *Protein Sci. 12*, 153−160.
(45) Robinson, D. R., and Jencks, W. P. (1965) The Effect of Compounds of the Urea-Guanidinium Class on the Activity Coefficient of Acetyltetraglycine Ethyl Ester and Related Compounds1. *J. Am. Chem. Soc. 87*, 2462−2470.
(46) Nozaki, Y., and Tanford, C. (1970) The solubility of amino acids, diglycine, and triglycine in aqueous guanidine hydrochloride solutions. *J. Biol. Chem. 245*, 1648−1652.
(47) Makhatadze, G. I., and Privalov, P. L. (1992) Protein interactions with urea and guanidinium chloride: A calorimetric study. *J. Mol. Biol. 226*, 491−505.
(48) Lim, W. K., Rösgen, J., and Englander, S. W. (2009) Urea, but not guanidinium, destabilizes proteins by forming hydrogen bonds to the peptide group. *Proc. Natl. Acad. Sci. U. S. A. 106*, 2595−2600.
(49) Myers, J. K., Pace, C. N., and Scholtz, J. M. (1995) Denaturant m values and heat capacity changes: relation to changes in accessible surface areas of protein unfolding. *Protein Sci. 4*, 2138−2148.
(50) Courtenay, E. S., Capp, M. W., Saecker, R. M., and Record, M. T. (2000) Thermodynamic analysis of interactions between denaturants and protein surface exposed on unfolding: Interpretation of urea and guanidinium chloride m-values and their correlation with changes in accessible surface area (ASA) using preferential interactio. *Proteins Struct. Funct. Bioinforma. 41*, 72−85.
(51) Arakawa, T., and Timasheff, S. N. (1984) Protein stabilization and destabilization by guanidinium salts. *Biochemistry 23*, 5924−5929.
(52) Yang, W. Y., Pitera, J. W., Swope, W. C., and Gruebele, M. (2004) Heterogeneous Folding of the trpzip Hairpin: Full Atom Simulation and Experiment. *J. Mol. Biol. 336*, 241−251.
(53) Aghera, N., Dasgupta, I., and Udgaonkar, J. B. (2012) A Buried Ionizable Residue Destabilizes the Native State and the Transition State in the Folding of Monellin. *Biochemistry 51*, 9058−9066.
(54) Zaidi, F. N., Nath, U., and Udgaonkar, J. B. (1997) Multiple intermediates and transition states during protein unfolding. *Nat. Struct Mol. Biol. 4*, 1016−1024.
(55) Sánchez, I. E., and Kiefhaber, T. (2003) Hammond Behavior versus Ground State Effects in Protein Folding: Evidence for Narrow Free Energy Barriers and Residual Structure in Unfolded States. *J. Mol. Biol. 327*, 867−884.
(56) Otzen, D. E., Kristensen, O., Proctor, M., and Oliveberg, M. (1999) Structural Changes in the Transition State of Protein Folding: Alternative Interpretations of Curved Chevron Plots. *Biochemistry 38*, 6499−6511.
(57) Llinas, M., Gillespie, B., Dahlquist, F. W., and Marqusee, S. (1999) The energetics of T4 lysozyme reveal a hierarchy of conformations. *Nat. Struct Mol. Biol. 6*, 1072−1078.
(58) Bédard, S., Mayne, L. C., Peterson, R. W., Wand, A. J., and Englander, S. W. (2008) The Foldon Substructure of Staphylococcal Nuclease. *J. Mol. Biol. 376*, 1142−1154.
(59) Hagen, S. J. (2007) Probe-dependent and nonexponential relaxation kinetics: Unreliable signatures of downhill protein folding. *Proteins Struct. Funct. Bioinforma. 68*, 205−217.
(60) Gruebele, M. (2008) Comment on probe-dependent and nonexponential relaxation kinetics: Unreliable signatures of downhill protein folding. *Proteins Struct. Funct. Bioinforma. 70*, 1099−1102.
(61) Liu, F., Du, D., Fuller, A. A., Davoren, J. E., Wipf, P., Kelly, J. W., and Gruebele, M. (2008) An experimental survey of the transition between two-state and downhill protein folding scenarios. *Proc. Natl. Acad. Sci. U. S. A. 105*, 2369−2374.
(62) Cho, S. S., Weinkam, P., and Wolynes, P. G. (2008) Origins of barriers and barrierless folding in BBL. *Proc. Natl. Acad. Sci. U. S. A. 2007*, 118−123.
(63) Liu, F., and Gruebele, M. (2007) Tuning lambda6−85 towards downhill folding at its melting temperature. *J. Mol. Biol. 370*, 574−84.
(64) Yang, W. Y., and Gruebele, M. (2004) Folding lambda-repressor at its speed limit. *Biophys. J. 87*, 596−608.
(65) Chen, T., and Chan, H. S. (2014) Effects of desolvation barriers and sidechains on local-nonlocal coupling and chevron behaviors in coarse-grained models of protein folding. *Phys. Chem. Chem. Phys. 16*, 6460−6479.
(66) Marcus, R. A. (1993) Electron transfer reactions in chemistry theory and experiment. *Rev. Mod. Phys. 65*, 251−259.


DOI: 10.1021/acs.biochem.5b00247
*Biochemistry* 2015, 54, 3431−3441